J. Membrane Biol. 129, 237–252 (1992)

The Journal of
Membrane Biology

Excitation-Contraction Coupling in a Pre-Vertebrate Twitch Muscle: The Myotomes of *Branchiostoma lanceolatum*

R. Benterbusch†, F.W. Herberg‡, W. Melzer†, and R. Thieleczek‡

†Lehrstuhl für Zellphysiologie, Ruhr-Universität Bochum, ND-4, D-4630 Bochum, Federal Republic of Germany, and ‡Institut für Physiologische Chemie, Abteilung für Biochemie Supramolekularer Systeme, Ruhr-Universität Bochum, MA-2, D-4630 Bochum, Federal Republic of Germany

Summary. The segmented trunk muscle (myotome muscle) of the lancelet (*Branchiostoma lanceolatum*), a pre-vertebrate chordate, was studied in order to gain information regarding the evolution of excitation-contraction (EC) coupling.

Myotome membrane vesicles could be separated on isopycnic sucrose gradients into two main fractions, probably comprising solitary microsomes and diads of plasma membrane and sarcoplasmic reticulum, respectively. Both fractions bound the dihydropyridine PN 200/110 and the phenylalkylamine (−)D888 (devapamil) while specific ryanodine binding was observed in the diad preparation only. Pharmacological effects on Ca^{2+} currents measured under voltage-clamp conditions in single myotome fibers included a weak block by the dihydropyridine nifedipine and a shift of the voltage dependences of inactivation and restoration to more negative potentials by (−)D888. After blocking the Ca^{2+} current by cadmium in voltage-clamped single fibers, the contractile response persisted and a rapid intramembrane charge movement could be demonstrated. Both responses exhibited a voltage sensitivity very similar to the one of the voltage-activated Ca^{2+} channels.

Our biochemical and electrophysiological results indicate that the EC coupling mechanism of the protochordate myotome cell is similar to that of the vertebrate skeletal muscle fiber: Intracellular Ca^{2+} release, presumably taking place via the ryanodine receptor complex, is under control of the cell membrane potential. The sarcolemmal Ca^{2+} channels might serve as voltage sensors for this process.

Key Words muscle · excitation-contraction coupling · ryanodine receptor · Ca^{2+} current · dihydropyridine receptor · Ca^{2+} release

Introduction

Vertebrate twitch muscle is designed for rapid nerve-controlled movement. An action potential propagates from the neuromuscular junction to the immediate vicinity of the contractile filaments via the transverse tubular (TT) system.[1] Voltage sensors in the membrane of the TT system receive the depolarization signal and control the release of messenger Ca^{2+} stored in the sarcoplasmic reticulum (SR), which turns on the contractile machinery by rapid binding to troponin C (Ashley, Mulligan & Lea, 1991; Rios & Pizarro, 1991). Two control mechanisms of Ca^{2+} release by cell membrane voltage have been proposed for vertebrate striated muscle. In heart muscle, Ca^{2+} release from the SR induced by Ca^{2+} inward flow through voltage-dependent L-type Ca^{2+} channels has been suggested (Fabiato, 1983; Sipido & Wier, 1991). For skeletal muscle a mechanism independent of this current flow could be demonstrated (Lüttgau & Spiecker, 1979; Brum, Rios & Stefani, 1988), which is nevertheless suppressed by L-type Ca^{2+} channel antagonists (Lüttgau, Böhle & Schnier, 1992). In both cases, the α_1 subunit of an L-type Ca^{2+} channel, the dihydropyridine (DHP) receptor, seems to be crucial for the functioning of EC coupling (Tanabe et al., 1990*a*, *b*). Tanabe et al. (1990*a*) expressed modified α_1 subunits of the heart in myotubes of dysgenic mice. The exchange of only the small segment which connects domains II and III

[1] *Abbreviations:* ASW, artificial sea water; DHP, dihydropyridine; DTE, dithioerythritol; EC coupling, excitation-contraction coupling; EDTA, ethylenediaminetetraacetic acid; EGTA, ethyleneglycol-bis(β-aminoethyl)-N,N,N′,N′-tetraacetic acid; HEPES, N-[2-hydroxyethyl]piperazine-N′-[2-ethanesulfonic acid]; HMM, heavy myotome microsomes; JFP, junctional foot protein; LMM, light myotome microsomes; PAGE, polyacrylamide gel electrophoresis; SDS, sodium dodecyl sulfate; SR, sarcoplasmic reticulum; TES, N-tris[hydroxymethyl]methyl-2-aminoethanesulfonic acid; Tris, tris(hydroxymethyl)aminomethane; TT system, transverse tubular system.

for the corresponding segment from skeletal muscle turned heart-type into skeletal-muscle-type EC coupling. It seems that the voltage sensor for EC coupling in striated muscle has evolved from a voltage-dependent Ca^{2+} channel which became interfaced in a still unknown way via its II–III loop to the SR Ca^{2+} release channel, i.e., the junctional foot protein (JFP) or ryanodine receptor (Block et al., 1988; Lai et al., 1987, 1988).

In this investigation we combined biochemical and electrophysiological techniques to study the myotome muscle of the protochordate *Branchiostoma lanceolatum* (the "lancelet"), which is thought to resemble an immediate ancestor of the vertebrates (for references *see* Dorit, Walker & Barnes, 1991). The fast twitch muscle of this organism exhibits features of both, heart-type and skeletal-muscle-type EC coupling. Its activation resembles heart-type EC coupling in terms of its sensitivity to extracellular Ca^{2+} (Hagiwara, Henkart & Kidokoro, 1971), but under certain conditions it has been shown to contract in the absence of external Ca^{2+} (Spiecker, Melzer & Lüttgau, 1979; Melzer, 1982*b*). Here we present evidence that the *Branchiostoma* twitch muscle exhibits a similar signal transfer mechanism between cell membrane and Ca^{2+} storage organelles as vertebrate skeletal muscle.

Materials and Methods

Lancelets (*B. lanceolatum*) were obtained from the Marine Biological Laboratory at Helgoland and were kept in sea water aquaria at temperatures between 14 and 20°C for up to a few months.

Preparation of Myotome Microsomes and Skeletal Muscle Triads

About 150 specimens (50–200 mg each) were used for a standard preparation of myotome membrane vesicles. After decapitation, the intestines and gonads were removed, leaving behind mainly the trunk musculature of the animal. This tissue was homogenized in ice-cold buffer containing (in mM) 250 sucrose, 2 DTE, 3 histidine, 5 EGTA-Tris, 0.2 EDTA-Tris, pH 7.5, and the protease inhibitors pepstatin (1 μM), leupeptin (1 μM), and phenylmethylsulfonyl fluoride (0.1 mM). Myotome microsomes (about 1 mg protein per g of specimen) were obtained from this crude homogenate by differential centrifugation following a procedure described for rabbit skeletal muscle (Caswell, Lau & Brunschwig, 1976). The microsomes were separated by centrifugation for 14 hr at 95,000 × *g* on a linear sucrose gradient (17 ml, 15–50% wt/wt sucrose) in a Sorvall AH 627 rotor. Gradient fractions (0.5 ml) were either kept on ice until further processing or stored at −70°C. Sucrose concentrations of the gradient fractions were measured by refractometry, and protein was determined according to Bradford (1976) using bovine serum albumin as a standard. All preparative steps were carried out at 4°C.

Skeletal muscle triads were prepared from rabbit back muscle according to Caswell et al. (1976) for comparative studies under identical experimental conditions. They were employed in control experiments at the same final concentrations as the myotome microsomes.

Gel Electrophoresis

Sodium dodecyl sulfate (SDS)-polyacrylamide gel electrophoresis (PAGE) was carried out according to Laemmli (1970), employing the following molecular mass standards: myosin, 200,000 kDa; β-galactosidase, 116,250 kDa; phosphorylase *b*, 97,400 kDa; and bovine serum albumin, 66,200 kDa. The gels were stained with either Coomassie blue R-250 (Laemmli, 1970), Stains-all (Campbell, MacLennan & Jorgensen, 1983) or silver (Wray et al., 1981).

Immunoblotting and Immunoprecipitation

Western blotting of proteins obtained from myotome microsomes and rabbit skeletal muscle triads (controls) to nitrocellulose (Schleicher & Schuell, BA 85) was carried out in a graphite plate electroblotting apparatus according to Kyhse-Andersen (1984) at a current of 200 mA for 2 hr. Blotting efficiencies estimated from staining patterns of gels before and after transblotting were ≥90% for polypeptides of $M_r \leq 200{,}000$ and about 60–80% for those of higher M_r. Immobilized polypeptides were detected immunologically as described by Towbin, Staehelin and Gordon (1979) using a peroxidase-conjugated biotin-extravidin system (Sigma) and employing antibodies at a dilution of 1 : 200. Polyclonal antibodies to calsequestrin (goat anti-rabbit skeletal muscle, rabbit anti-bovine heart muscle) were gifts from Dr. M. Michalak, Edmonton, Canada. Antibodies to the JFP of skeletal muscle (polyclonal rabbit anti-rabbit, monoclonal mouse anti-rabbit coupled to sepharose 4b) were generously supplied by Dr. A. H. Caswell, Miami, FL. The sepharose-coupled monoclonal antibodies to the JFP were employed in immunoprecipitation experiments to detect cross-reacting epitopes on polypeptides of myotome microsomes. A portion (1 mg) of either myotome microsomes or skeletal muscle triads (controls) was solubilized for 90 min at room temperature in 1 ml buffer (1 M NaCl, 1 mM EGTA, 0.1% Zwittergent 3–14 (Calbiochem), 2 mM histidine, pH 7.5) containing 0.2 ml of the sepharose-coupled antibody. The assay was centrifuged for 10 min at 3,200 × *g*, and the sediment was washed three times with the above buffer containing 4 M NaCl. The resulting sediment was suspended in 1 mM EGTA, 10 mM Tris, pH 7.5, and centrifuged again. The final sediment was suspended in 0.1 ml sample buffer (Laemmli, 1970) and incubated for 7 min at 100°C, which led to the dissociation of the antibody antigen complex. An aliquot (30 μl) of this sample was subjected to SDS-PAGE according to Laemmli (1970).

Ca^{2+} Transport ATPase Activity and Ca^{2+} Accumulation

The distribution of Ca^{2+} transport ATPase activity throughout a sucrose gradient with separated myotome microsomes was determined flourimetrically according to Brandt (1985) using 4-methylumbelliferyl phosphate (Boehringer). Total ATPase activity was measured in the presence of 1 mM free Mg^{2+} and 3μM free Ca^{2+}; Ca^{2+}-independent ATPase activity was determined at 1 mM free

Mg^{2+} in the absence of added Ca^{2+}. The assays were carried out in 0.5 ml buffer (50 mM KCl, 2 mM EGTA, 2 mM DTE, 5 μM 4-methylumbelliferyl phosphate, 10 mM TES, pH 7.5), containing an aliquot of the gradient fractions (10–50 μg protein) and appropriate concentrations of $MgCl_2$ and $CaCl_2$ calculated using the affinity constants of EGTA given by Fabiato and Fabiato (1979) and Fabiato (1985). The difference between the two measured activities provided the distribution of Ca^{2+}-dependent ATPase activity of myotome microsomes.

Ca^{2+} accumulation by myotome microsomes was determined in the presence of oxalate according to Caswell et al. (1976). Myotome microsomes (250 μl) were incubated for 45 min in 250 mM sucrose, 3 mM histidine, 5 mM oxalate, 10 mM ATP, 11 mM $MgCl_2$, 50 μM $CaCl_2$ (10^4 Bq $^{45}CaCl_2$/ml), 20 mM Tris-HCl, pH 7.7. The Ca^{2+}-loaded microsomes were separated by isopycnic sucrose density centrifugation as described before, and the protein and the radioactivity distribution throughout the sucrose gradient were determined. Microsomes incubated without ^{45}Ca were run in parallel as control.

Ca^{2+} Release from Myotome Microsomes

Agonist-induced Ca^{2+} release from myotome microsomes was determined at room temperature essentially as described by Meissner and Henderson (1987). Microsomes (5 mg) were sedimented by centrifugation at 100,000 × *g* in buffer A (100 mM KCl, 20 mM TES-KOH, 0.1 mM EGTA, 0.1 mM $CaCl_2$, pH 7.0) for 45 min. The pellet was resuspended in 0.8 ml buffer A containing 1 mM $CaCl_2$ (2×10^5 Bq $^{45}CaCl_2$/ml). After 2 hr of incubation, 50 μl of this sample were mixed with 0.5 ml of buffer B (100 mM KCl, 20 mM TES-KOH, 1 mM EGTA, 0.2 mM $CaCl_2$, 1 mM $MgCl_2$, pH 7.0). Ca^{2+} release was initiated after 10 sec by adding 1 ml of release solution (buffer B containing no additives or either 5 mM AMP or 5 mM caffeine). Aliquots (0.4 ml) were removed from the assays 10, 40, and 70 sec after mixing and were rapidly vacuum filtrated through nitrocellulose filters (Schleicher & Schuell, BA 85). The filters were washed three times with 2 ml ice-cold buffer C (100 mM KCl, 20 mM TES-KOH, 0.5 mM $MgCl_2$, 0.1 mM EGTA, 10 μM ruthenium red, pH 7.0), and the radioactivity remaining on the filters, which represents the intraluminal Ca^{2+}, was determined by scintillation counting. Maximum Ca^{2+} release was determined with Mg^{2+}-free buffer B containing 5 mM AMP and 5 mM caffeine instead of the release solution. To monitor the basal Ca^{2+} content of myotome microsomes at the times indicated, buffer C was added instead of the release solution.

Ryanodine Binding

Ryanodine binding to myotome microsomes was determined essentially as described by Michalak, Dupraz and Shoshan-Barmatz (1988). Light or heavy myotome microsomes (46 μg each) were incubated for 2 hr at 37°C in 0.2 ml of an optimized binding buffer (1 M NaCl, 250 mM sucrose, 2 mM DTE, 50 μM $CaCl_2$, 20 mM 2-[N-morpholino]ethanesulfonic acid, pH 6.5) containing different concentrations of [^{3}H]ryanodine (New England Nuclear) as indicated. Nonspecific ryanodine binding, determined at each [^{3}H]ryanodine dose in the presence of 1000-fold excess of unlabeled ligand, was on the order of 20–40% of total binding. Bound and free ryanodine were separated by gel filtration according to Inui, Saito and Fleischer (1987). The assays were applied to PD-10 columns (Pharmacia) and eluted with binding buffer. Eluted fractions containing protein were combined and the amounts of co-eluted radioligand were determined from aliquots of these samples by scintillation counting.

Binding of PN 200/110 and (−)D888

The assay of PN 200/110 binding to myotome microsomes was carried out under dim red light. Light or heavy myotome microsomes (60–100 μg in 50 μl) were added to 250 μl binding buffer (150 mM KCl, 50 mM Tris-HCl, pH 7.4) containing different concentrations of (+)-[5-methyl-^{3}H]-PN 200/110 (New England Nuclear) as indicated. The assays were incubated for 1 hr at room temperature. Nonspecific binding was determined at each concentration of radioligand in presence of 1000-fold excess of unlabeled nifedipine (Calbiochem). Bound and free ligand were separated by vacuum filtration of the assays through glass fiber filters (Whatman GF/C) followed by three washes with 5 ml ice-cold binding buffer. Bound ligand was determined by scintillation counting of the filters.

Binding of (−)D888 to myotome microsomes was assayed at daylight but otherwise as described for PN 200/110, except that the binding buffer was composed of 150 mM KCl, 1 mM EGTA, 10 mM TES-KOH, pH 7.4. The concentrations of (−)-[^{3}H]-desmethoxy verapamil, [^{3}H](−)D888, (Amersham) were as indicated in the figure legends. Nonspecific ligand binding was determined at each dose of [^{3}H](−)D888 in the presence of 1000-fold excess of unlabeled (−)D888 (Amersham). The glass fiber filters were pretreated for 1 hr in 0.5% polyethylenimine (Sigma) in order to minimize ligand binding to the filters (Dumont et al., 1988).

Solutions for Electrophysiological Experiments

The methods used in electrophysiological experiments on myotome cells have been described previously (Benterbusch & Melzer, 1992). Artificial sea water (ASW), used for the dissection of specimens and isolation of single cells, contained (in mM) 400 NaCl, 10 KCl, 10 $CaCl_2$, 50 $MgCl_2$, 10 HEPES, pH 7.5. The pipette solution for intracellular perfusion contained (in mM) 410 Cs, 20 Na, 10.3 Mg, 4 ATP, 10 HEPES, 420 aspartate, 40 Cl, 1 EGTA, pH 7.3. When the EGTA concentration was changed to 10 or 0.2 mM, the Mg concentration was changed correspondingly to 12.3 or 10.1 mM, maintaining free Mg^{2+} at 4 mM according to the equilibrium constants given by Fabiato and Fabiato (1979) and Fabiato (1985). The external solution which was designed to minimize ionic conductance pathways other than Ca^{2+} channels contained 410 mM tetraethylammonium, 10 mM Ca, 50 mM Mg, 10 mM HEPES, 520 mM methane sulfonate ($CH_3SO_3^-$), 3.1 μM tetrodotoxin, pH 7.5. Deviations from the given compositions are noted at appropriate places in Results. The experiments were carried out at room temperature if not explicitly stated.

Single Cell Isolation

The size of the specimens used for electrophysiological investigations ranged from 14 to 35 mm. After transfer to ASW and decapitation, the ventral body wall, the viscera, and the surface epithelium were removed. The preparation was transferred to ASW containing 10 mg/ml Collagenase A (Boehringer). After 120 to 165 min at 21°C, the notochord and nerve chord were removed from the muscle and the myotomes were dissociated into single cells

by gentle shaking in enzyme-free ASW. We recorded from band-shaped cells or cell fragments (myotome fibers, Benterbusch & Melzer, 1992) which ranged in length between 130 and 390 μm and in width between 7 and 12 μm. According to electron microscopic studies, myotome cells have a thickness of about 1 μm (Flood, 1968; Grocki, 1982).

Voltage Clamping, Data Acquisition, and Analysis

For voltage clamping we used suction electrodes in the whole-cell configuration and an EPC-7 patch-clamp amplifier (List). Signals were digitized using a DA-AD converter board (DT 2821-F-16SE, Data Translation) in a IBM-AT 286-compatible microcomputer. Each digital record consisted of 960 consecutive data values sampled at 5 to 15 kHz. Currents recorded at depolarizing voltage pulses were corrected for linear leak and capacitive currents by adding an appropriately scaled current average obtained by applying 3–7 small hyperpolarizing control pulses before and after each test pulse at intervals between 0.7 and 0.8 sec.

Recording of Cell Movement

Mechanical activation of cells stimulated by depolarization was detected optically as a shortening response. The inverted microscope (Olympus IMT2) used for the experiments was equipped with a photomultiplier set-up (microscope photometer SF, Zeiss), which recorded the light in a circular field of the object plane. The end of the cell-stripe was placed into this field so that shortening caused an increase in light intensity, which was approximately proportional to the extent of shortening.

Results

Isolation and Characterization of Myotome Microsomes

Separation of microsomes isolated from myotomes of the lancelet by isopycnic sucrose density gradient centrifugation led to the characteristic protein distribution shown in Fig. 1. This protein profile is considerably different from the one obtained with skeletal muscle microsomes isolated and separated under virtually identical conditions (Caswell et al., 1976; Varsanyi et al., 1986). Two main microsomal fractions could be distinguished (Fig. 1*A*): Light myotome microsomes (LMM) at 27 ± 1.5% (wt/wt) sucrose and heavy myotome microsomes (HMM) at 33 ± 2% (wt/wt) sucrose. SDS-PAGE of sucrose gradient fractions (Fig. 1*B*) revealed in both LMM and HMM the presence of a high molecular mass polypeptide of slightly higher electrophoretic mobility than the JFP of skeletal muscle triads under comparable conditions (lane *T*). In the skeletal muscle triad preparation this protein was identified as the JFP by immunoblotting with polyclonal antibodies

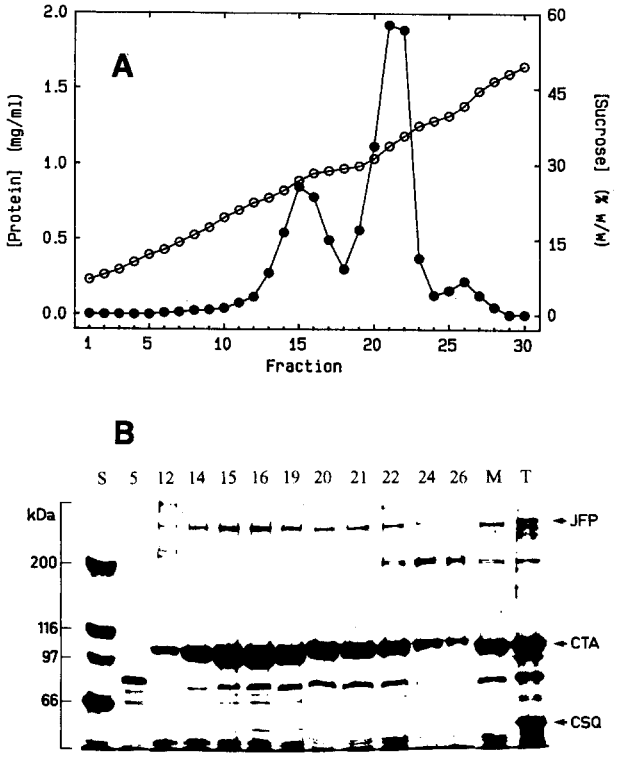

Fig. 1. Fractionation of myotome microsomes and separation of microsomal proteins. (*A*) Representative example of a total number of 16 microsome preparations. Myotome microsomes (6.5 mg) were subjected to isopycnic sucrose gradient centrifugation (filled circles: protein distribution; open circles: sucrose concentration). (*B*) SDS-PAGE on 6% polyacrylamide gels of aliquots (10 μl) from selected fractions (indicated above the lanes) of the gradient shown in *A*. The lanes marked by *M*, *T*, and *S* contained myotome microsomes (20 μg), rabbit skeletal muscle triads (20 μg), and standard proteins of indicated molecular masses (10 μg, *see* Materials and Methods), respectively. *JFP*, *CTA*, and *CSQ* mark junctional foot protein, SR Ca^{2+} transport ATPase, and calsequestrin of skeletal muscle, respectively. The apparent M_r of the JFP determined with the molecular mass standards employed is on the order of 340,000; its true M_r is 565,000 as derived from cDNA cloning (Takeshima et al., 1989).

against JFP. The distribution of the JFP in the sucrose gradient correlated with the distribution of the predominant protein of myotome microsomes of M_r 105,000 (lane *T*). This protein most likely represents the Ca^{2+} transport ATPase of the SR (MacLennan et al., 1985). In agreement with this interpretation, Ca^{2+}-dependent ATPase activity and active Ca^{2+} accumulation was found in LMM as well as in HMM (*not shown*). A band corresponding to a third characteristic major protein of skeletal muscle triads, calsequestrin (lane *T*), was not detectable in myotome microsomes. Other staining techniques suitable for detecting calsequestrin (Stains-all, silver) or immunoblotting with polyclonal antibodies to

calsequestrin of rabbit skeletal muscle gave no hints at the presence of this Ca^{2+} storage protein in myotomes either. Yet, polyclonal antibodies to calsequestrin of bovine heart muscle showed cross-reaction with a minor protein band of about M_r 85,000 (*not shown*). The polyclonal antibody to the JFP of rabbit skeletal muscle (*see above*) did not cross-react with any polypeptide of myotome microsomes. Moreover, immunoprecipitation of solubilized myotome microsomes with monoclonal antibodies to the JFP (which avoided SDS-PAGE and protein blotting prior to immunodetection, *see* Materials and Methods) did not reveal cross-reacting domains on myotome polypeptides either (*not shown*).

Ryanodine Receptors and Agonist-Stimulated Ca^{2+} Release

From ryanodine binding and Ca^{2+} release experiments as shown in Fig. 2 it can be concluded that *Branchiostoma* myotomes have a functional Ca^{2+} release channel with similar characteristics as that of vertebrate skeletal muscles. Despite the appearance of a protein band corresponding to the JFP in LMM as well as in HMM (Fig. 1*B*), significant specific ryanodine binding was observed only with HMM. A maximum ryanodine binding capacity B_{max} of about 4.1 ± 0.1 pmol/mg and a dissociation constant K_D = 13.9 ± 3 nM was obtained (Fig. 2*A* and *see* Table 2). The corresponding data obtained with rabbit skeletal muscle triads under the same experimental conditions were B_{max} = 19.8 ± 3.6 pmol/mg, K_D = 20.4 ± 0.3 nM (*see* Table 2). Agonists like caffeine or AMP, which are known to open the Ca^{2+} release channel of skeletal muscle SR (Meissner & Henderson, 1987), act on myotome microsomes analogously (Fig. 2*B*). The Ca^{2+} storage capacity of myotome microsomes estimated in the presence of ruthenium red was in the range of 10 nmol/mg which was significantly less than the apparent SR Ca^{2+} capacity measured in triads (50–90 nmol/mg).

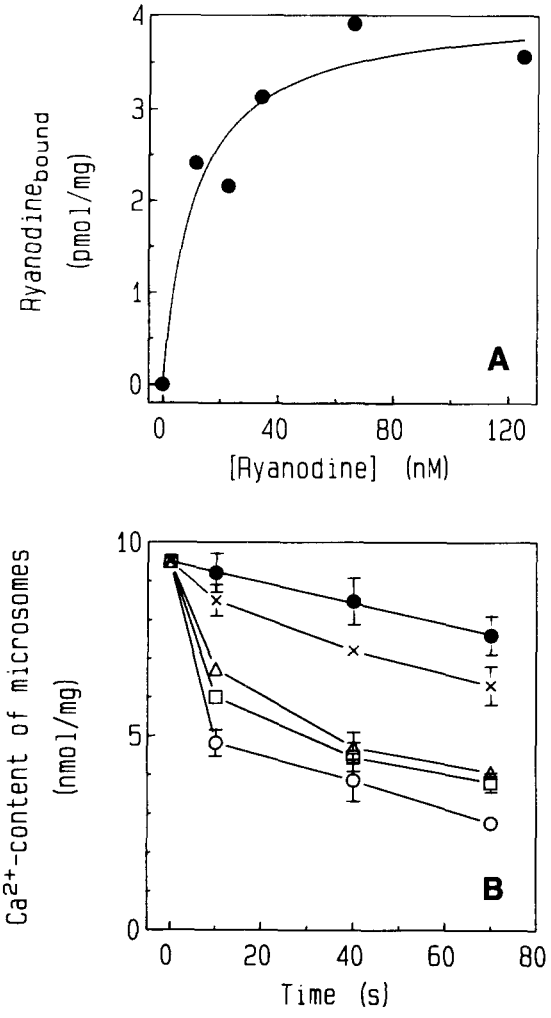

Fig. 2. Specific ryanodine binding to HMM (*A*) and agonist-induced Ca^{2+} release from myotome microsomes (*B*). The binding assay contained 0.23 mg/ml of HMM. A binding isotherm, $Ryanodine_{bound} = B_{max} \times [Ryanodine]/(K_D + [Ryanodine])$, was fitted to the data by nonlinear regression, yielding B_{max} = 4.1 pmol/mg and K_D = 10.9 nM. The Ca^{2+} content of myotome microsomes (0.15 mg/ml) was monitored in release solution (crosses) and in release solution containing 6.5 μM ruthenium red (filled circles), 3.2 mM AMP (open triangles), 3.2 mM caffeine (open squares), and 3.2 caffeine and 3.2 mM AMP (open circles), respectively. The bars indicate the scatter of the experimental data.

Calcium Antagonist Binding

The binding of drugs known to act on L-type Ca^{2+} channels was studied with LMM and HMM. The dihydropyridine PN 200/110 (Fig. 3 and *see* Table 2) bound with equally high affinities to sites present in LMM (K_D = 18.3 ± 0.8 nM, B_{max} = 5.7 ± 2.3 pmol/mg) as well as in HMM (K_D = 17.7 ± 0.8 nM, B_{max} = 3.8 ± 1.6 pmol/mg). Binding studies with the phenylalkylamine (−)D888 suggest the existence of two different binding sites (Fig. 4 and *see* Table 2). (−)D888 was bound to LMM with about three times lower affinity (K_D = 48.7 ± 5.7 nM, B_{max} = 11.3 ± 4.6 pmol/mg) and to HMM with about three times higher affinity (K_D = 6.8 ± 0.4 nM, B_{max} = 4.5 ± 1.4 pmol/mg) than PN 200/110. The curved Scatchard plot (indicated by the dashed curve in Fig. 4*C*) suggests a second (−)D888 binding site in HMM with about the same affinity of the site in LMM.

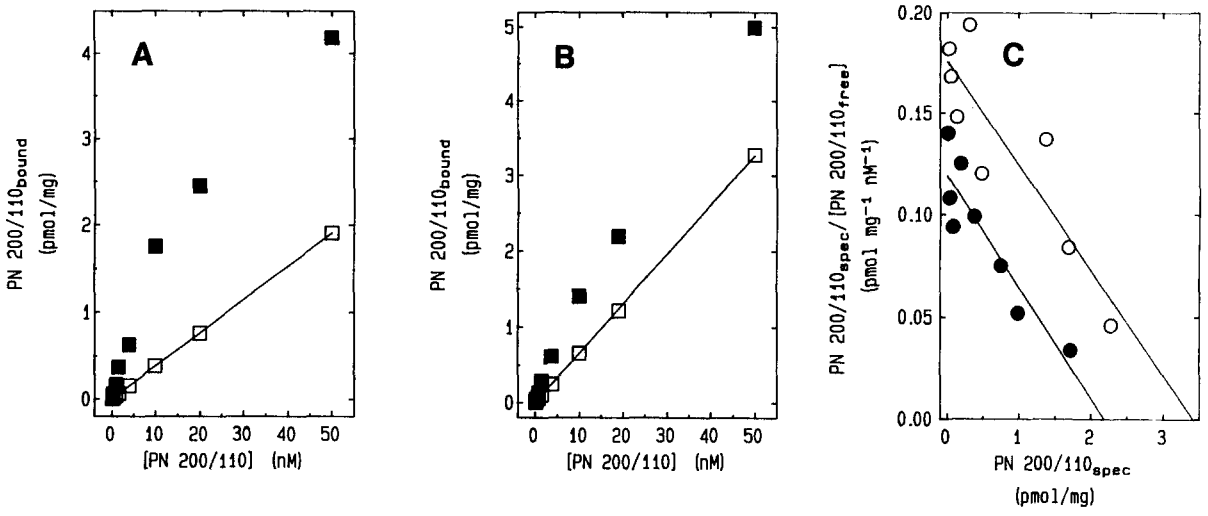

Fig. 3. Binding of PN 200/110 to myotome microsomes. Total binding (filled squares) and nonspecific binding (open squares) to LMM is shown in (*A*) and corresponding binding to HMM is shown in (*B*). The binding assays contained 0.26 mg/ml of LMM or 0.33 mg/ml of HMM. Specific binding (PN $200/110_{spec}$) was obtained by subtracting nonspecific from total binding. Scatchard analysis (*C*) of the data obtained with LMM (open circles) and with HMM (filled circles) yielded values for K_D and B_{max} of 19.5 nM and 3.4 pmol/mg for LMM and of 18.5 nM and 2.2 pmol/mg for HMM.

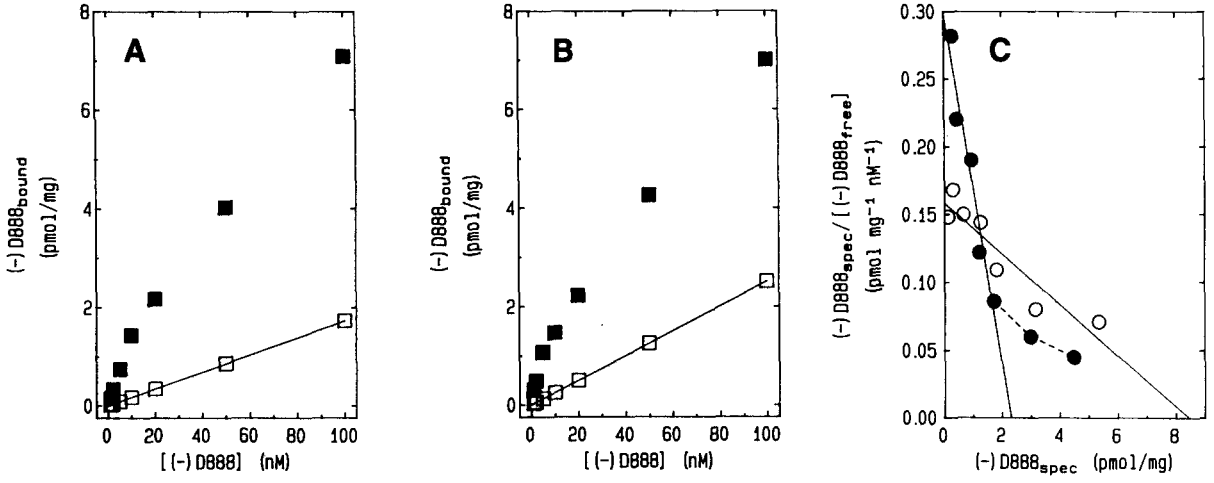

Fig. 4. Binding of (−)D888 to myotome microsomes. Total binding (filled squares) and nonspecific binding (open squares) to LMM is shown in (*A*) and corresponding binding to HMM is shown in (*B*). The binding assays contained 0.23 mg/ml of LMM or 0.25 mg/ml of HMM. Specific binding ($D888_{spec}$) was obtained by subtracting nonspecific from total binding. For Scatchard analysis (*C*) the data obtained with LMM (open circles) as well as those obtained with HMM (filled circles) up to 20 nM (−)D888 were approximated by linear regression. The obtained values for K_D and B_{max} were 53.2 nM and 8.4 pmol/mg for LMM and 7.7 nM and 2.3 pmol/mg for HMM.

Ca^{2+} Currents

In skeletal muscle, the opening of the Ca^{2+} release channels in the SR is possibly linked to a depolarization-induced conformational change of the DHP-sensitive transverse tubular Ca^{2+} channel (Tanabe et al., 1988; Lamb, 1991). Therefore, the Ca^{2+} current may provide information about conformational changes of the molecule that controls Ca^{2+} release and force generation. We found two kinetically distinct components in the Ca^{2+} currents in myotomes. A detailed investigation of the kinetic characteristics of these currents has been described elsewhere (Benterbusch & Melzer, 1992). In particular, it has been shown that the two phases are probably generated by only one channel population undergoing transient Ca^{2+}-dependent inactivation. Here our interest was focussed on the pharmacological sensitivity of the Ca^{2+} channels and the comparison of their voltage sensitivity to that of contractile activation.

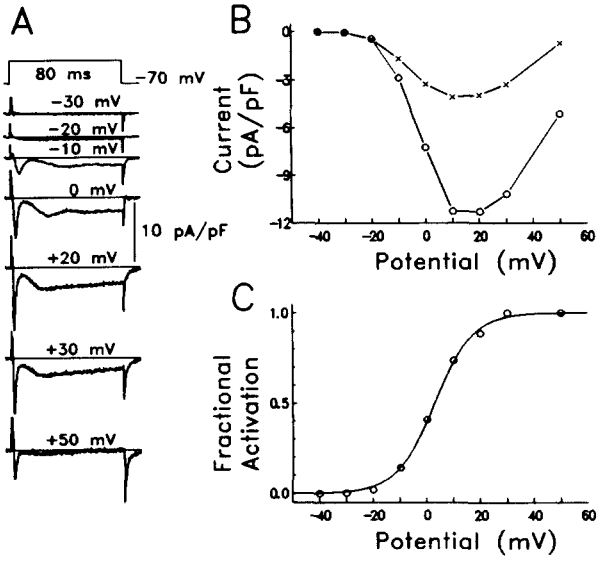

Fig. 5. Voltage-dependent Ca^{2+} currents in a myotome cell. (*A*) Currents recorded at different depolarizing potentials. (*B*) Peak values of the currents (including more records than shown in *A*) plotted against the pulse potential (crosses: slow phase; circles: fast phase). (*C*) Activation curve for voltage-dependent gating derived from the plot in *B* (fast phase), assuming that the current values at +30 and +50 mV represent the fully activated channel state. The current-voltage relation at these two potentials was linearly extrapolated to more negative potentials to obtain the open state current-voltage relation. The Boltzmann fit parameters (*see* text) were $V_{0.5} = 2.82$ mV and $k = 7.14$ mV. Experiment 75, C = 91 pF.

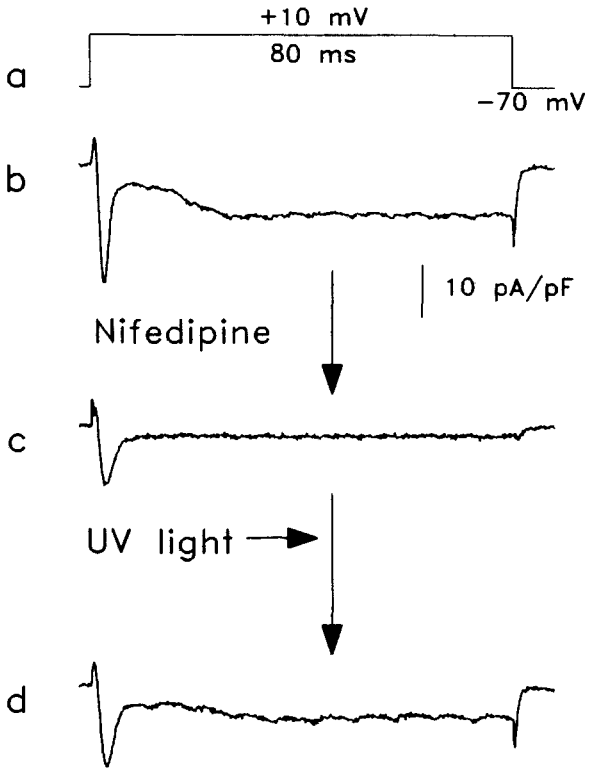

Fig. 6. Effect of nifedipine on the Ca^{2+} inward current in a myotome cell. (*a*) Voltage change; (*b*) control (internal EGTA: 10 mM); (*c*) 290 sec after changing to an external solution containing 30 μM nifedipine; and (*d*) recording after 50 sec of irradiation by a mercury arc lamp (Osram HBO 150). Experiment 112, C = 69 pF, 24°C.

Figure 5*A* shows the current response for step depolarizations of increasing amplitudes and Fig. 5*B* shows the current-voltage relation of the fast and the slow component. The activation curve in Fig. 5*C* was derived from the *I–V* relationship of the fast component. This curve represents a least-squares fit of a Boltzmann relation describing the voltage-dependent equilibrium between a resting (nonconducting) state and an active (open) state:

$$F = 1/(1 + \exp((V_{0.5} - V)/k))$$

where F is the fractional activation, V the membrane voltage, $V_{0.5}$ the voltage leading to half-maximal activation, and k a parameter determining the steepness of the curve (voltage sensitivity). The mean values obtained from eight experiments carried out under identical conditions were $V_{0.5} = -0.8 \pm 5.2$ mV and $k = 8.1 \pm 0.9$ mV.

Calcium Antagonist Effects

Both current components were affected by dihydropyridine and phenylalkylamine calcium antagonists, yet at considerably higher concentrations than the skeletal muscle L-type Ca^{2+} current. Figure 6 shows the effect of 30 μM nifedipine on the biphasic Ca^{2+} inward current. Photoinactivation of nifedipine (Morad, Goldman & Trentham, 1983; Gurney, Nerbonne & Lester, 1985; Neuhaus, Rosenthal & Lüttgau, 1990) by irradiating the cell with UV light led to partial recovery of the signal.

Phenylalkylamines act on skeletal muscle by stabilizing the depolarization-induced refractory state of the Ca^{2+} release mechanism and of the slow L-type Ca^{2+} channel (Pizarro et al., 1988; Feldmeyer, Melzer & Pohl, 1990). The measurable effects include a considerably slower restoration from inactivation after repolarization and a shift to more negative potentials of the curves describing steady-state inactivation or restoration as a function of voltage (Berwe, Gottschalk & Lüttgau, 1987; Erdmann & Lüttgau, 1989). To test the effect of the phenylalkylamine (−)D888 on myotome Ca^{2+} current we carried out the inactivation and restoration procedures which are schematically shown in the insets of Fig. 7. A concentration of 2.5 μM (−)D888 was

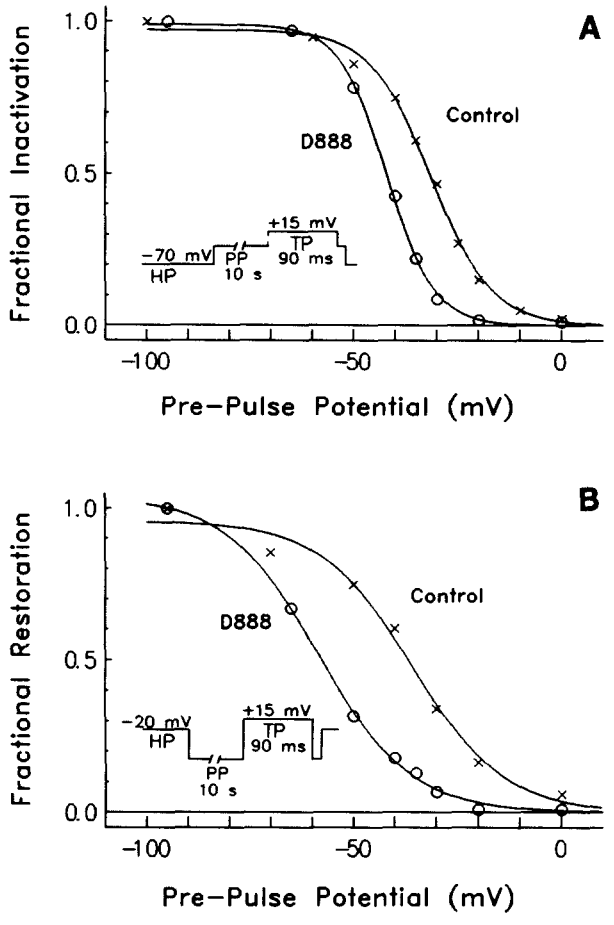

Fig. 7. Effect of (−)D888 on the voltage dependence of inactivation (*A*) and restoration (*B*). Representative data obtained under control conditions (crosses) and in the presence of 2.5 μM (−)D888 (open circles), respectively. (*A*) Inactivation caused by a 10-sec depolarization from a steady holding potential (*HP*) of −70 mV to various potentials (*PP*). The degree of inactivation was tested in each case by a fixed depolarizing step to +15 mV (*TP*). The relative peak current (fast phase) obtained at the test pulse is plotted against the prepulse potential. The slow phase was equally affected by conditioning depolarization. (*B*) Restoration measured after at least 60 sec at *HP* = −20 mV, which caused more than 80% inactivation under control conditions. After applying a 10-sec prepulse (*PP*) to various potentials, the degree of restoration was tested by a fixed step to +15 mV. The maximum current obtained at this test pulse (*TP*) is plotted against the restoration potential during the prepulse.

used which shows a strong effect on frog muscle (Erdmann & Lüttgau, 1989). A shift to more negative potentials caused by (−)D888 can be seen in both, the voltage dependence of inactivation (Fig. 7*A*) and of restoration (Fig. 7*B*). To quantify the effect, the fractional inactivation (or restoration) as a function of voltage was fitted individually for each experiment by a Boltzmann relation (*see* the Equation). The free parameters $V_{0.5}$ and k are shown in Table 1. When comparing the averages of the $V_{0.5}$ values, a shift of −13.2 mV caused by (−)D888 can be noticed in both voltage dependences. These results indicate that the Ca^{2+} channels of the plasma membrane are the drug receptors found in the myotome microsome preparation.

Figure 8 shows the effect of the phenylalkylamine (±)D600 (gallopamil), which is known to act like (−)D888 (yet at 10 to 100 times higher concentrations) on the tetanic force development of a small multicellular bundle dissected from the myotome muscle. The tetanic force production of the myotome strip at the stimulation rate of 50/sec, which is normally maintained for several seconds, turned into a phasic response. This change indicates a use-dependent suppression of force in the presence of (±)D600. It was partially reversible after the washout of (±600). At a low stimulation rate (1 per min), the same concentration of (±)D600 had no effect on twitch force. A half-maximal suppression of tetanic force (measured 1 sec after the onset of stimulation) was observed at about 40 μM.

Voltage Dependence of Mechanical Activation

In skeletal muscle, the control of intracellular Ca^{2+} release depends on cell membrane voltage and does not require the influx of Ca^{2+}. Previous work has shown that action potential-induced twitches are blocked in *Branchiostoma* myotomes after removing external Ca^{2+} (Hagiwara et al., 1971). However, twitches could be recovered in Ca^{2+}-free solutions (Spiecker et al., 1979; Melzer, 1982*b*), indicating a release of internal Ca^{2+}. To investigate the voltage dependence of contraction under voltage clamp, we used the unloaded shortening of the cell strips (recorded optically, *see* Materials and Methods) as an indicator of a rise in intracellular Ca^{2+}. Figure 9*A* shows the mechanical response to increasing depolarization in a bathing solution that contained no calcium but 2 mM cadmium. The contractile response shows a sigmoidal voltage dependence (Fig. 9*B*). This demonstrates that the myotome cells possess a mechanism for Ca^{2+} current-independent voltage-controlled force activation similar to that found in vertebrate skeletal muscle. The voltage dependence could be well fitted by a Boltzmann distribution (the Equation). Assuming that the mechanical response is proportional to the number of voltage sensors in the active state, the steepness of the activation curve (k = 8 mV) indicates the transfer of three elementary charges across the electrical field of the membrane

Table 1. Effect of 2.5 μM (−)D888 on voltage dependence of inactivation and restoration of the calcium current[a]

	Control	(−)D888
Inactivation	$V_{0.5}$ = −29.4 ± 5.6 mV (n = 9) k = −6.0 ± 1.8 mV	$V_{0.5}$ = −42.6 ± 1.5 mV (n = 4) k = −5.5 ± 0.3 mV
Restoration	$V_{0.5}$ = −38.5 ± 3.2 mV (n = 5) k = −7.0 ± 2.1 mV	$V_{0.5}$ = −51.7 ± 6.1 mV (n = 6) k = −9.2 ± 2.1 mV

[a] The pulse protocols shown in the insets of Fig. 7 were applied to a number (n) of different cells and the fractional peak inward current obtained at the test pulse as a function of the prepulse voltage was fitted by the Equation. Tabulated are the mean values (±SD). The main effect of (−)D888 was a shift of the voltage dependence to more negative potentials, notable as a more negative value of the fit parameter $V_{0.5}$. According to a variance analysis (Bortz, 1979), the differences are significant at an error probability of 0.0001.

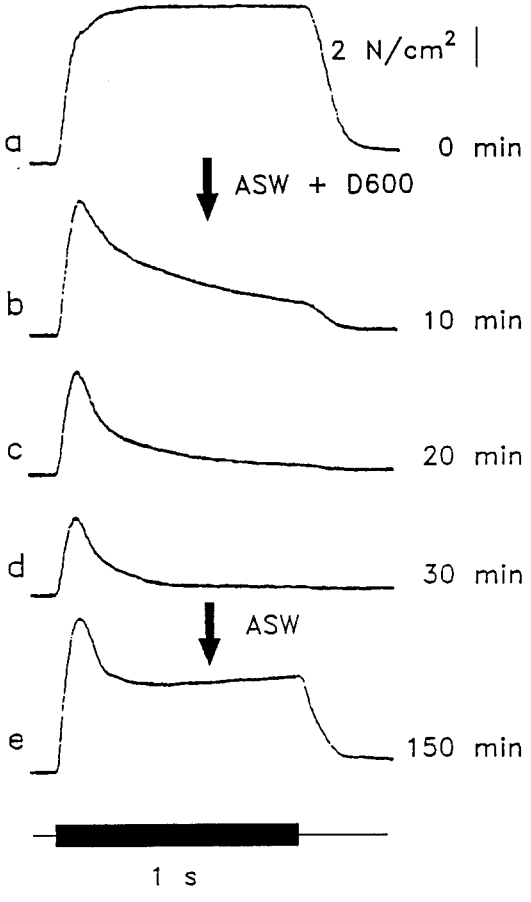

Fig. 8. Effect of (±)D600 on tetanic force development in a small strip (about 3 mm long and 0.3 mm thick) dissected from a myotome muscle. During the period indicated by the thick line (bottom) the muscle was stimulated extracellularly at 50 Hz for 1 sec using platinum plate electrodes. (*a*) Control (in ASW); (*b–d*) Consecutive tetani elicited in ASW containing 100 μM (±)D600 at 10-min intervals; and (*e*) partial recovery of tetanic force development after a 2-hr wash in drug-free ASW. The ASW in this experiment contained 10 mM Tris (pH = 8.0) instead of HEPES. The temperature was 10°C.

during the state change of the voltage sensor. Very similar activation characteristics were obtained from the voltage dependence of the peak Ca^{2+} inward current (Fig. 5). Comparable sigmoidal curves for contractile activation were obtained in the standard external solution containing 10 mM Ca^{2+} (the Boltzmann fit parameters $V_{0.5}$ (mV) and k (mV) were −5.0 and 7.2 for one experiment at −70 mV holding potential and averaged −8.2 and 7.5 for two experiments at −37 mV). A quantification of absolute differences in the maximum contractile response obtained was not possible due to limitations of the recording method.

Although contractions were possible in the absence of external Ca^{2+}, they could only be maintained for a certain period of time in the whole-cell recording mode. Run-down occurred in both, Ca^{2+}-containing and Ca^{2+}-free external solutions, but the contractile response appeared to be more labile in the Ca^{2+}-free cadmium-containing solution. This may have been due to the progressive depletion of the Ca^{2+} stores or to an irreversible run-down of EC coupling. Occasionally, when measuring Ca^{2+} currents, a visual inspection of the cell gave the impression that contraction was weaker at strong depolarization, particularly later in the experiment. Therefore, it cannot be ruled out that Ca^{2+} influx makes an additional contribution to contractile activation, which may become discernible when internally releasable Ca^{2+} is depleted. We found no steady inhibition of microscopically visible movement by (−)D888, suggesting that no drastic suppression of restoration from inactivation of the voltage-sensing mechanism for EC coupling occurred. Our method would not permit observing relatively small effects of (−)D888 on the movement signal of the isolated cell comparable to those on the current.

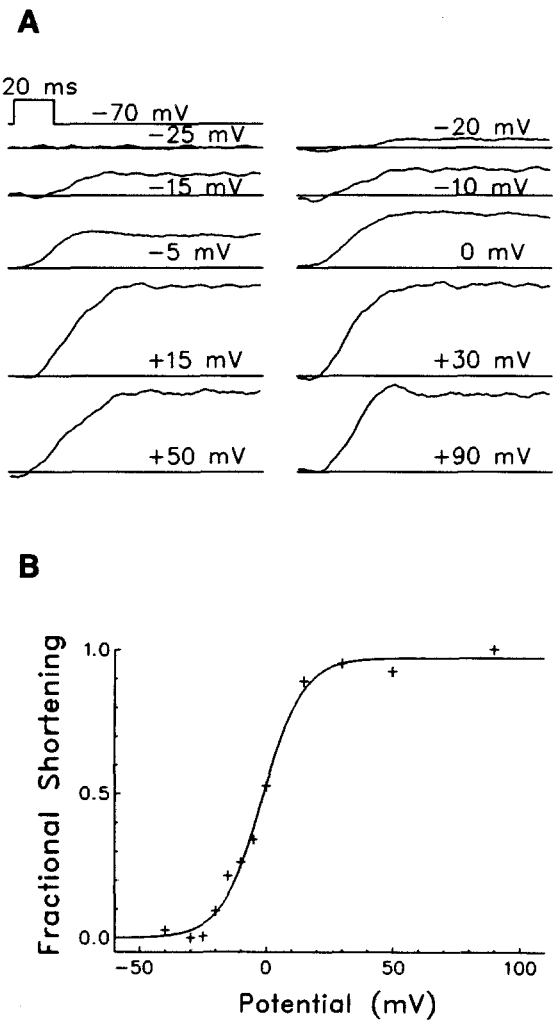

Fig. 9. Voltage-dependent contractile activation of a myotome cell. (*A*) Depolarizations of 20-msec duration to the potentials indicated at each record were applied while unloaded shortening was detected using a light-sensing device (*see* Materials and Methods). (*B*) Maximal contractile response plotted against pulse potential. The continuous line is a least-squares fit of a Boltzmann relation (the Equation) to the data points. Fit parameters: $V_{0.5}$ = −1.5 mV, k = 8.0 mV. The external solution contained no Ca and 2 mM Cd but only 10 mM tetraethylammonium and 400 mM Na; $CH_3SO_3^-$ was replaced by Cl^-; this improved survival of the cells in the Ca^{2+}-free solution. The internal solution contained 0.2 mM EGTA. Experiment 132, C = 60 pF, 24°C.

Intramembrane Charge Movements

We also searched for a voltage-sensor signal associated with the contractile and current activation. The charge of the intramembrane unit which is necessary to sense the depolarization, should generate a transient intramembrane current at the turn-on and turn-off of the depolarizing pulse that should become visible when all ionic currents are blocked (Schneider & Chandler, 1973). Little ionic current remained under the conditions used for our experiments when 1 mM $CdCl_2$ was added to the solution. Figure 10 shows the residual currents measured under these conditions at the onset of various depolarizing pulses and when stepping back to the holding potential of −70 mV after 80 msec. In fact, these currents show the properties expected from an intramembrane charge displacement. The voltage dependence (Fig. 10*C*) of the charge displacement showed a sigmoidal relationship, which could be well fitted by a Boltzmann relation (the Equation, with $F = Q/Q_{max}$). The maximum charge displacement (Q_{max}) per linear capacitance determined in two fibers which exhibited little ionic current and a clear saturation at positive potentials was 10.6 and 13.1 nC/μF (on) and 9.4 and 11.4 nC/μF (off).

In the fiber of Fig. 10 the complete I–V relation of the Ca^{2+} current could be determined prior to the application of cadmium. The activation curve for the inward current (*compare* Fig. 5) was very similar to the charge-voltage relation obtained in the presence of cadmium. At pulse-on the values for k were 7.7 mV (current) and 7.8 mV (charge), which correspond to the movement of about three elementary charges across the membrane per unitary voltage-sensor reaction. The $V_{0.5}$ values were −8.2 and −10.9 mV, respectively. Soon after reaching the peak the intramembrane current declined exponentially. As expected for a simple voltage-dependent transition between two states, the on time constants showed a bell-shaped voltage dependence, exhibiting a maximum value of 1.7 msec very close to the turn-over point of the charge-voltage relation ($V_{0.5}$). The time constants of the off-transients varied only slightly from 0.34 msec at the −40-mV pulse to 0.58 msec at the +50-mV pulse.

Discussion

The muscle cell morphology of *Branchiostoma* deviates from vertebrate skeletal muscle in that the cells are not cylindrical fibers but thin lamellae containing only a single layer of myofibrils and virtually no TT system (Flood, 1968; Grocki, 1982). Therefore, they exhibit the junctions between cell membrane and SR on their surface (Fig. 11).

The microsomes which could be prepared from *Branchiostoma* myotomes showed a similar distribution on sucrose density gradients as those obtained from rabbit heart muscle (Varsanyi et al., 1986). The lighter of the two microsomal fractions of heart was assigned to solitary SR vesicles and the heavier fraction to diads (Varsanyi et al., 1986). Considering the morphology of the myotome cell

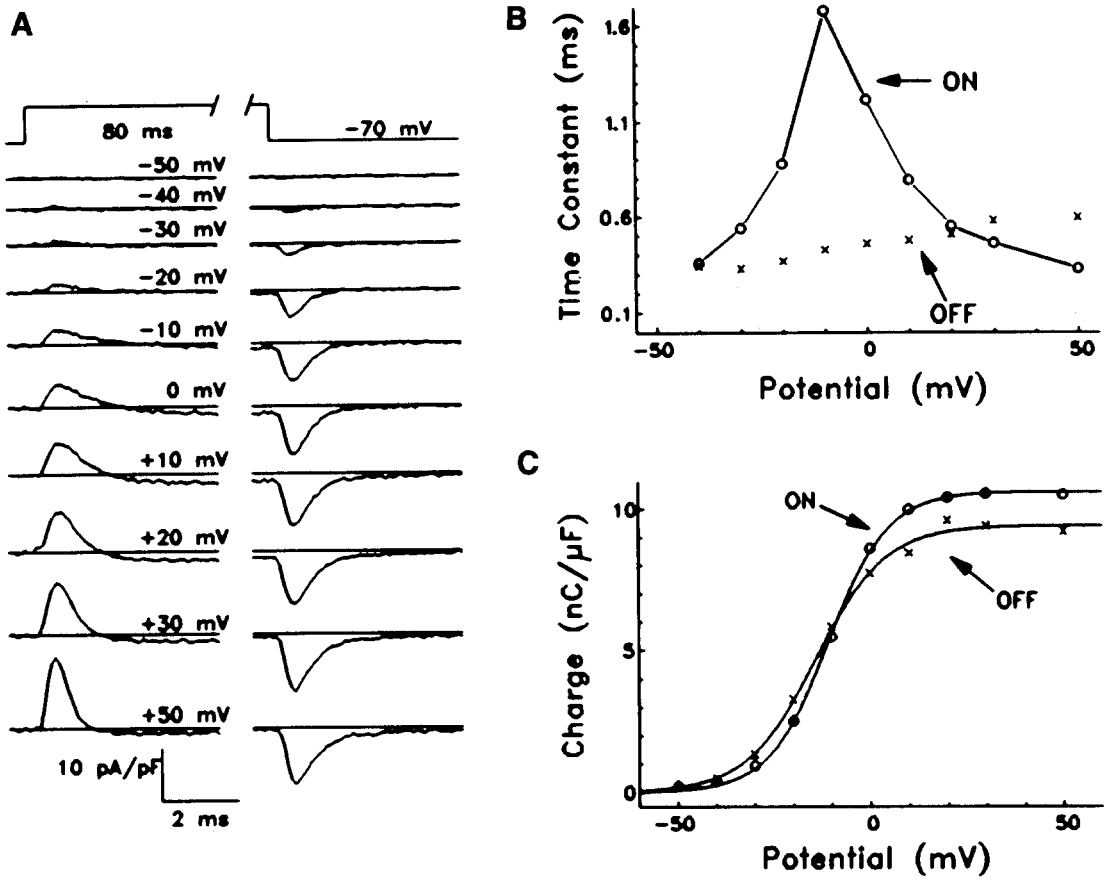

Fig. 10. Nonlinear intramembrane charge movements in a myotome cell. (*A*) Nonlinear current measured during the first 5 msec after the onset (on-response) of 80-msec pulses to various potentials and during the first 5 msec after stepping back to the holding potential (off-response). (*B*) Time constants determined by fitting a single exponential function plus a constant to the declining phase of the transient currents shown in *A*. (*C*) Intramembrane mobile charge estimated by integrating on- and off-responses over the first 4.5 msec following the potential change after subtracting the small current value at the end of this time interval. Experiment 77, C = 77 pF, 22.5°C.

(Fig. 11), formation of solitary sarcolemmal and SR microsomes (LMM) as well as of sarcolemma/SR-diads (HMM) during preparation of myotome microsomes appears to be likely. The putative SR Ca^{2+} transport protein, Ca^{2+}-dependent ATPase activity, and Ca^{2+} accumulation were found in LMM and HMM, confering SR-like characteristics to both microsomal fractions. The Ca^{2+} channel antagonists PN 200/110 and (−)D888 bound with high affinity to sites in LMM as well as in HMM, indicating also the presence of sarcolemmal receptors in both myotome membrane fractions (Table 2). A polypeptide of similar molecular mass as the monomer of the SR Ca^{2+} release channel (ryanodine receptor) of vertebrate skeletal muscle (Lai et al., 1987, 1988; Block et al., 1988; Takeshima et al., 1989) was detected in LMM and HMM. However, high-affinity ryanodine binding could be measured only with HMM, i.e., with presumably intact plasma membrane-SR complexes. Caffeine-induced Ca^{2+} release from myotome microsomes was observed at concentrations effective also in vertebrate skeletal muscles (Meissner & Henderson, 1987; Herrmann-Frank, 1989). These observations suggest that like in skeletal muscle, the detected ryanodine receptors establish a functional Ca^{2+} release channel in the SR of myotome cells. The low-affinity, high-capacity Ca^{2+}-binding protein calsequestrin located in terminal cisternae of skeletal muscle SR, which has been suggested to play a role in the regulation of Ca^{2+} release (Ikemoto et al., 1989), could neither be detected in microsomes nor in crude homogenates of myotomes. This protein seems to be present in all tetrapodes (MacLennan, Campbell & Reithmeier, 1983) but was not found in carp muscles either (Dux et al., 1989).

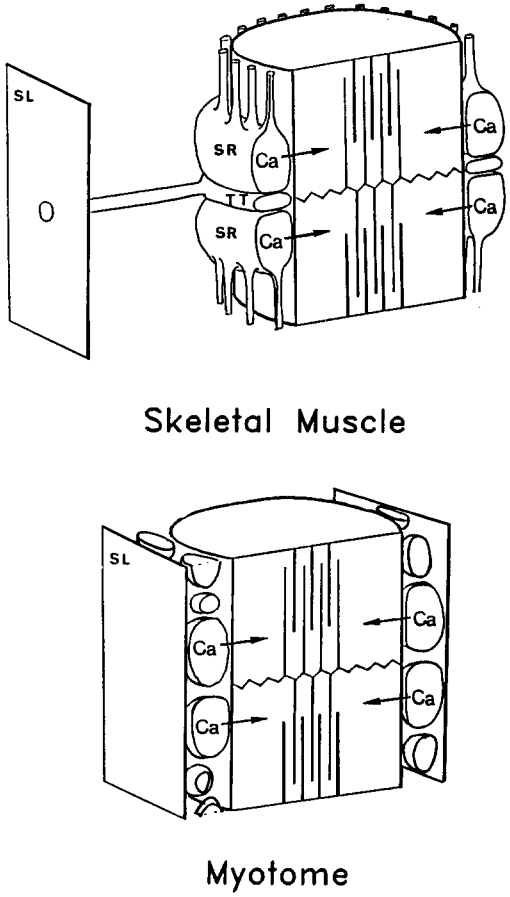

Fig. 11. Schematic structure of a myofibril and the associated membranous elements involved in EC coupling in frog skeletal muscle (top) and the myotome cell of *Branchiostoma* (bottom). *SL:* sarcolemma; *SR:* sarcoplasmic reticulum; *TT:* transverse tubule. The arrows indicate Ca^{2+} release during muscle activation.

Table 2 summarizes the main results of the biochemical and physiological experiments and compares the data concerning *Branchiostoma* myotomes with those obtained from vertebrate skeletal muscle. The myotome shares a number of features with a fast twitch skeletal muscle. In particular, a voltage-controlled release of intracellularly stored Ca^{2+} is present. This confirms earlier conclusions based on twitch measurements in Ca^{2+}-free solutions (Spiecker et al., 1979; Melzer, 1982*b*).

The voltage dependence of mechanical activation corresponds well to that of the intramembrane charge movement signal. Charge movement relaxation kinetics is somewhat faster than in skeletal muscle, exhibiting a maximum time constant of less than 2 msec compared to more than 3 msec at the same temperature in rat skeletal muscle fibers (Simon & Beam, 1985*a,b*). It seems likely that the voltage-sensor signal for Ca^{2+} release is part of this rapid charge movement. On the other hand, the voltage dependence and kinetics of the intramembrane charge movements are compatible with a role of this signal in gating the fast Ca^{2+} current. As has been suggested for skeletal muscle (Lamb & Walsh, 1987), they may control both events simultaneously.

The charge movements received little contribution from a rapidly immobilizing component because the off-charge after 80-msec pulses was at least 87% of the on-charge. The steepness of the charge-voltage relation and of the voltage dependence of Ca^{2+} conductance activation both indicate independently moving units of about three elementary charges (equivalent to about 4.8×10^{-10} nC). The specific membrane capacitance of myotome cells is close to 1 $\mu F/cm^2$ (Melzer, 1982*a*; Benterbusch & Melzer, 1992). The total density of a mobile nonlinear charge of 11 $nC/\mu F$ leads to an estimate of 2.29×10^{10} reactive units per cm^2 cell surface membrane involved in charge movement.

Henkart, Landis and Reese (1976) and Grocki (1982) described electron-dense particles in the 11- to 15-nm gap between sarcolemma and subsarcolemmal vesicles in the muscle cells of *Branchiostoma*. These particles had a similar appearance as the junctional feet in vertebrate skeletal muscle (Franzini-Armstrong, 1975). With their center-to-center distance of 34 to 38 nm and their regular square arrangement, a number of 7.72×10^{10} of these structures is available per cm^2 junctional area. Since the junctions cover about 20% of the cell surface (Flood, 1977) the average "foot density," referring to the total cell surface, is $154/\mu m^2$. When comparing this value to the density of charge-carrying units derived from the charge-voltage relation (s.a.), one obtains 1.49 voltage-sensing units per "foot." This is close to the ratio of two DHP receptors per Ca^{2+} release channel in skeletal muscle given the structural arrangement proposed by Block et al. (1988) and would be consistent with an involvement of most of the charges in EC coupling. A lower ratio can be estimated from the binding studies with ryanodine, PN 200/110, and (−)D888 carried out on diads. The binding capacity of diads for ryanodine was about 4.1 pmol/mg, whereas the one for PN 200/110 and (−)D888 was in the range of 3.8–4.5 pmol/mg (Table 2). From these values a ratio of 0.9–1.1 DHP receptors per Ca^{2+} release channel can be calculated for *Branchiostoma* myotomes.

The "foot" density in the cell membrane of the myotome is about five times less than the value of 790 per μm^2 of T-system surface reported for frog skeletal muscle (Franzini-Armstrong, 1975). It should be noted that, due to the higher surface-to-volume ratio (1–2 $\mu m^2/\mu m^3$) in myotomes, the volume density of junctional "feet" and therefore presumptive Ca^{2+} release channels is similar in the

Table 2. Structural and functional qualities of EC coupling in *Branchiostoma* myotomes and vertebrate skeletal muscles

	Myotome	Skeletal
Ca current		
Activation	fast	slow
Half-maximal inhibition by nifedipine	>10 μM	<1 μM[a]
Shift of inactivation by phenylalkylamines	weak	strong
Intramembrane charge movement	fast	fast
EC coupling		
External Ca necessary	no	no
Effect of phenylalkylamines		
inhibition of tetanus	yes (D600)	no (D888)
Paralysis	no	yes
Sarcoplasmic reticulum		
Interaction with cell membrane	diads	triads
Ca release control by cell membrane potential	yes	yes
Ca release by caffeine	yes	yes
Ca storage capacity (nmol/mg)	≈10	50–90[b]
Calsequestrin present	no	yes
DHP receptor		
Binding of PN 200/110 to LMM		
K_D (nM)	18.3 ± 0.8(3)[c]	2.9 ± 1.3(2)[b,c]
B_{max} (pmol/mg)	5.7 ± 2.3(3)[c]	8.7 ± 1.3(2)[b,c]
Binding of PN 200/110 to HMM		
K_D (nM)	17.7 ± 0.8(3)[c]	
B_{max} (pmol/mg)	3.8 ± 1.6(3)[c]	
Binding of (−)D888 to LMM		
K_D (nM)	48.7 ± 5.7(4)[c]	2.2[d]
B_{max} (pmol/mg)	11.3 ± 4.6(4)[c]	18.0[d]
Binding of (−)D888 to HMM		
K_D (nM)	6.8 ± 0.4(4)[c]	
B_{max} (pmol/mg)	4.5 ± 1.4(4)[c]	
Ryanodine receptor		
Ryanodine binding		
K_D (nM)	13.9 ± 3.0(2)[c]	20.4 ± 0.3(2)[b,c]
B_{max} (pmol/mg)	4.1 ± 0.1(2)[c]	19.8 ± 3.6(2)[b,c]
Apparent M_r of JFP	≈330,000[e]	≈340,000[b,e]

[a] From Lamb and Walsh (1987).
[b] Obtained with rabbit skeletal muscle triads under identical experimental conditions.
[c] Values are the mean ± SE; the number of replicates is given in parentheses.
[d] From Goll et al. (1984), obtained with partially purified T-tubules of guinea pig skeletal muscle.
[e] Determined with the molecular mass standards employed (*see* Fig. 1*B*).

myotome (1.5–3 × 10^{17} per liter cell volume) and in skeletal muscle (1.7 × 10^{17} per liter fiber volume; Franzini-Armstrong, 1975).

Our results indicate that the Ca^{2+} channels of the myotome cell membrane are receptors for dihydropyridines and phenylalkylamines. On the other hand, binding and physiological effects of these drugs are weaker in myotomes than in skeletal muscles (Erdmann & Lüttgau, 1989). Phenylalkylamines paralyze skeletal muscle fibers by strongly retarding restoration and shifting steady-state restoration of force to more negative potentials (40 mV at 2.5 μM (−)D888). Ca^{2+} current restoration is affected in a similarly strong way (Berwe et al., 1987; Pizarro et al., 1988; Erdmann & Lüttgau, 1989; Feldmeyer et al., 1990). We found two binding sites for (−)D888 in myotome microsomes with dissociation constants of about 6.8 and 48.7 nM, respectively (Table 2). The

first one obtained from putative diads exhibited a similar affinity as the single binding site which has been reported for skeletal muscle T-tubules (K_D = 2.2 nM, Goll et al., 1984). Selective binding of the drug to the inactive state of the myotome Ca^{2+} channel (Bean, 1984; Erdmann & Lüttgau, 1989) would predict a shift of the voltage dependence of inactivation and restoration as has been observed. However, with the available data an assignment of binding sites to particular states of the channel appears premature. A use-dependent action on EC coupling might be inferred from the D600 effect on tetani in multicellular myotome strips (Fig. 8). In skeletal muscle use-dependent paralysis by phenylalkylamines could only be demonstrated for depolarization-induced contractures but not for tetani (Lüttgau et al., 1992).

In summary, intracellular Ca^{2+} release in *Branchiostoma* myotome cells, presumably taking place via the ryanodine receptor complex, is under control of the cell membrane potential. The mode of EC coupling postulated for heart muscle (Ca^{2+}-current-induced Ca^{2+} release) can be ruled out as the sole mechanism for EC coupling since voltage-dependent activation can be found in the absence of a Ca^{2+} inward current. The structures that bind calcium antagonists (DHP receptors) are voltage-dependent Ca^{2+} channels. However, while in principle the voltage-control mechanism of internal Ca^{2+} release in skeletal muscle and myotome appears to be similar, one notices a number of differences (Table 2) which may reflect the evolutionarily older state of the myotome system. It seems conceivable that the evolution of EC coupling proceeded from voltage-controlled influx of external Ca^{2+} to voltage-controlled internal Ca^{2+} release. Twitch muscles of the scorpion seem to have conserved an EC coupling mechanism in which the Ca^{2+} current (gated by a rapid charge movement) is essential for contractile activation (Scheuer & Gilly, 1986). One may speculate that *Branchiostoma* represents a further step of the evolutionary process: The sarcolemmal Ca^{2+} channels are still rapidly opened but communicate additionally with the internal Ca^{2+} release channel like in vertebrate skeletal muscle. In the latter the sarcolemmal Ca^{2+} channels have lost the ability to open rapidly and contractile activation is achieved exclusively by the newly developed interaction leading to release of internal Ca^{2+}.

The morphology of the myotome cells allows direct access to the junctions between cell membrane and SR on the cell surface (Fig. 11). Therefore, local activation experiments might be feasible similar to those carried out by Huxley and Taylor (1958). Such experiments may complement attempts to reconstitute the native interaction between the membrane of the TT system and the SR membrane in skeletal muscle and may provide new insights into the layout of the voltage-dependent Ca^{2+} release mechanism.

We thank Drs. H.Ch. Lüttgau and L.M.G. Heilmeyer, Jr. for stimulating discussions during the work, Dr. N.R. Brandt for helpful suggestions, and Drs. A.H. Caswell and M. Michalak for their generous gifts of antibodies. We also thank Ms. P. Goldmann, Mr. R. Schwalm, and Mr. U. Siemen for technical support and Ms. E. Linnepe for editorial help. This work was supported by grant Gl 72/1-5 of the Deutsche Forschungsgemeinschaft. R. Benterbusch was recipient of a scholarship by the Studienstiftung des Deutschen Volkes.

References

Ashley, C.C., Mulligan, I.P., Lea, T.J. 1991. Ca^{2+} and activation mechanisms in skeletal muscle. *Q. Rev. Biophys.* **24:**1–73

Bean, B.P. 1984. Nitrendipine block of cardiac calcium channels: High-affinity binding to the inactivated state. *Proc. Natl. Acad. Sci. USA* **81:**6388–6392

Benterbusch, R., Melzer, W. 1992. Ca^{2+} current in myotome cells of the lancelet (*Branchiostoma lanceolatum*). *J. Physiol.* **450:**437–453

Berwe, D., Gottschalk, G., Lüttgau, H.C. 1987. Effects of the calcium antagonist gallopamil (D600) upon excitation-contraction coupling in toe muscle fibres of the frog. *J. Physiol.* **385:**693–707

Block, B.A., Imagawa, T., Campbell, K.P., Franzini-Armstrong, C. 1988. Structural evidence for direct interaction between the molecular components of the transverse tubule/sarcoplasmic reticulum junction in skeletal muscle. *J. Cell Biol.* **107:**2587–2600

Bortz, J. 1979. Lehrbuch der Statistik. Springer-Verlag, Berlin

Bradford, M.M. 1976. A rapid and sensitive method for the quantitation of microgram quantities of protein utilizing the principle of protein-dye binding. *Anal. Biochem.* **72:**248–254

Brandt, N.R. 1985. Identification of two populations of cardiac microsomes with nitrendipine receptors: Correlation of the distribution of dihydropyridine receptors with organelle specific markers. *Arch. Biochem. Biophys.* **242:**306–319

Brum, G., Rios, E., Stefani, E. 1988. Effects of extracellular calcium on calcium movements of excitation-contraction coupling in frog skeletal muscle fibres. *J. Physiol.* **398:**441–473

Campbell, K.P., MacLennan, D.H., Jorgensen, A.O. 1983. Staining of Ca^{2+} binding proteins, calsequestrin, calmodulin, troponin C, and S-100, with the cationic carbocyanine dye "Stains-all." *J. Biol. Chem.* **258:**11267–11273

Caswell, A.H., Lau, Y.H., Brunschwig, J.-P. 1976. Ouabain-binding vesicles from skeletal muscle. *Arch. Biochem. Biophys.* **176:**417–430

Dorit, R.L., Walker, W.F., Barnes, R.D. 1991. Zoology. pp. 804–813. Sounders College Publishing, Philadelphia

Dumont, L., Williams, J.S., Vaghy, P.L., Schwartz, A. 1988. Characteristics of the phenylalkylamine binding site in canine cardiac sarcolemmal membranes. *Basic Res. Cardiol.* **83:**369–375

Dux, L., Lelkes, G., Hieu, L.H., Nemcsok, J. 1989. Structural differences between the Ca^{2+}-ATPase enzymes of sarcoplasmic reticulum membrane from rabbit and carp muscles. *Comp. Biochem. Physiol.* **92B:**263–270

Erdmann, R., Lüttgau, H.C. 1989. The effect of the phenyl-

alkylamine D888 (devapamil) on force and Ca^{2+} current in isolated frog skeletal muscle fibres. *J. Physiol.* **413:**521–541

Fabiato, A. 1983. Calcium-induced release of calcium from the cardiac sarcoplasmic reticulum. *Am. J. Physiol.* **245:**C1–C14

Fabiato, A. 1985. Time and calcium dependence of activation and inactivation of calcium-induced release of calcium from the sarcoplasmic reticulum of a skinned canine carciac Purkinje cell. *J. Gen. Physiol.* **85:**247–289

Fabiato, A., Fabiato, F. 1979. Calculator programs for computing the composition of the solutions containing multiple metals and ligands used for experiments in skinned muscle cells. *J. Physiol. (Paris)* **75:**463–505

Feldmeyer, D., Melzer, W., Pohl, B. 1990. Effects of gallopamil on calcium release and intramembrane charge movements in frog skeletal muscle fibres. *J. Physiol.* **421:**343–362

Flood, P.R. 1968. Structure of the segmental trunk muscle in *Amphioxus*. *Z. Zellforschung* **84:**389–416

Flood, P.R. 1977. The sarcoplasmic reticulum and associated plasma membrane of trunk muscle lamellae in *Branchiostoma lanceolatum (Pallas)*. *Cell Tissue Res.* **181:**169–196

Franzini-Armstrong, C. 1975. Membrane particles and transmission at the triad. *Fed. Proc.* **34:**1382–1389

Goll, A., Ferry, D.R., Striessnig J., Schober, M., Glossmann, H. 1984. (−)-[^{3}H]Desmethoxyverapamil, a novel Ca^{2+} channel probe. *FEBS Lett.* **176:**371–377

Grocki, K. 1982. The fine structure of the deep muscle lamellae and their sarcoplasmic reticulum in *Branchiostoma lanceolatum*. *Eur. J. Cell Biol.* **28:**202–212

Gurney, A.M., Nerbonne, J.M., Lester, H.A. 1985. Photoinduced removal of nifedipine reveals mechanisms of calcium antagonist action on single heart cells. *J. Gen. Physiol.* **86:**353–379

Hagiwara, S., Henkart, M.P., Kidokoro, Y. 1971. Excitation-contraction coupling in *Amphioxus* muscle cells. *J. Physiol.* **219:**233–251

Henkart, M., Landis, D.M.D., Reese, T.S. 1976. Similarity of junctions between plasma membranes and endoplasmic reticulum in muscle and neurons. *J. Cell. Biol.* **70:**338–347

Herrmann-Frank, A. 1989. Caffeine- and Ca^{2+}-induced mechanical oscillations in isolated skeletal muscle fibres of the frog. *J. Muscle Res. Cell Motil.* **10:**437–445

Huxley, A.F., Taylor, R.E. 1958. Local activation of striated muscle fibres. *J. Physiol.* **144:**426–441

Ikemoto, N., Ronjat, M., Meszaros, L.G., Koshita, M. 1989. Postulated role of calsequestrin in the regulation of calcium release from sarcoplasmic reticulum. *Biochemistry* **28:**6764–6771

Inui, M., Saito, A., Fleischer, S. 1987. Purification of the ryanodine receptor and identity with the feet structures of terminal cisternae of sarcoplasmic reticulum from fast skeletal muscle. *J. Biol. Chem.* **262:**1740–1747

Kyhse-Andersen, J. 1984. Electroblotting of multiple gels: A simple apparatus without buffer tank for rapid transfer of proteins from polyacrylamide to nitrocellulose. *J. Biochem. Biophys. Methods* **10:**203–209

Laemmli, U.K. 1970. Cleavage of structural proteins during the assembly of the head of bacteriophage T4. *Nature* **227:**680–685

Lai, F.A., Erickson, H.P., Block, B.A., Meissner, G. 1987. Evidence for a junctional feet-ryanodine receptor complex from sarcoplasmic reticulum. *Biochem. Biophys. Res. Commun.* **143:**704–709

Lai, F.A., Erickson, H.P., Rousseau, E., Liu, Q.Y., Meissner, G. 1988. Purification and reconstitution of the calcium release channel from skeletal muscle. *Nature* **331:**315–319

Lamb, G.D. 1991. Ca^{2+} channels or voltage sensors? *Nature* **352:**113

Lamb, G.D., Walsh, T. 1987. Calcium currents, charge movement and dihydropyridine binding in fast- and slow-twitch muscles of rat and rabbit. *J. Physiol.* **393:**595–617

Lüttgau, H.C., Böhle, T., Schnier, A. 1992. Ca^{2+} antagonists as tools in the analysis of excitation-contraction coupling in skeletal muscle fibres. *In:* Excitation-Contraction Coupling in Skeletal, Cardiac, and Smooth Muscle. G.B. Frank, C.P. Bianchi, and H. TerKeurs, editors. Plenum, New York *(in press)*

Lüttgau, H.C., Spiecker, W. 1979. The effects of calcium deprivation upon mechanical and electrophysiological parameters in skeletal muscle fibres of the frog. *J. Physiol.* **296:**411–429

MacLennan, D.H., Brandl, C.J., Korczak, B., Green, N.M. 1985. Aminoacid sequence of a Ca^{2+} + Mg^{2+}-dependent ATPase from rabbit muscle sarcoplasmic reticulum, deduced from its complementary DNA sequence. *Nature* **316:**696–700

MacLennan, D.H., Campbell, K.P., Reithmeier, R.A.F. 1983. Calsequestrin. *In:* Calcium and Cell Function. A. Martonosi, editor. Vol. 4, pp. 151–173. Academic, New York

Meissner, G., Henderson, J.S. 1987. Rapid calcium release from cardiac sarcoplasmic reticulum vesicles is dependent on Ca^{2+} and is modulated by Mg^{2+}, adenine nucleotide, and calmodulin. *J. Biol. Chem.* **262:**3065–3073

Melzer, W. 1982*a*. Electrical membrane properties of the muscle lamellae in *Branchiostoma* myotomes. *Eur. J. Cell Biol.* **28:**213–218

Melzer, W. 1982*b*. Twitch activation in Ca^{2+}-free solutions in the myotomes of the lancelet (*Branchiostoma lanceolatum*). *Eur. J. Cell Biol.* **28:**219–225

Michalak, M., Dupraz, P., Shoshan-Barmatz, V. 1988. Ryanodine binding to sarcoplasmic reticulum membrane; comparison between cardiac and skeletal muscle. *Biochim. Biophys. Acta* **939:**587–594

Morad, M., Goldman, Y.E., Trentham, D.R. 1983. Rapid photochemical inactivation of Ca^{2+} antagonists shows that Ca^{2+} entry directly activates contraction in frog heart. *Nature* **304:**635–638

Neuhaus, R., Rosenthal, R., Lüttgau, H.C. 1990. The effects of dihydropyridine derivates on force and Ca^{2+} current in frog skeletal muscle fibres. *J. Physiol.* **427:**187–209

Pizarro, G., Brum, G., Fill, M., Fitts, R., Rodriguez, M., Uribe, I., Rios, E. 1988. The voltage sensor of skeletal muscle excitation-contraction coupling: A comparison with Ca^{2+} channels. *In:* The Calcium Channel: Structure, Function and Implications. M. Morad, W. Nayler, S. Kazda, and M. Schramm, editors. pp. 138–156. Springer-Verlag, Berlin

Rios, E., Pizzaro, G. 1991. Voltage sensor of excitation-contraction coupling in skeletal muscle. *Physiol. Rev.* **71:**849–907

Scheuer, T., Gilly, W.F. 1986. Charge movement and depolarization-contraction coupling in arthropod *vs.* vertebrate skeletal muscle. *Proc. Natl. Acad. Sci. USA* **83:**8799–8803

Schneider, M.F., Chandler, W.K. 1973. Voltage dependent charge movement in skeletal muscle: A possible step in excitation-contraction coupling, *Nature* **242:**244–246.

Simon, B.J., Beam, K.G. 1985*a*. Slow charge movement in mammalian skeletal muscle. *J. Gen. Physiol.* **85:**1–19

Simon, B.J., Beam, K.G., 1985*b*. The influence of transverse tubular delays on the kinetics of charge movement in mammalian skeletal muscle. *J. Gen. Physiol.* **85:**21–42

Sipido, K.R., Wier, W.G. 1991. Flux of Ca^{2+} across the sarcoplas-

mic reticulum of guinea-pig cardiac cells during excitation-contraction coupling. *J. Physiol.* **435:**605–630

Spiecker, W., Melzer, W., Lüttgau, H.Ch. 1979. Extracellular Ca^{2+} and excitation-contraction coupling. *Nature* **280:** 158–160

Takeshima, H., Nishimura, S., Matsumoto, T., Ishida, H., Kangawa, K., Minamino, N., Matsuo, H., Ueda, M., Hanaoka, M., Hirose, T., Numa, S. 1989. Primary structure and expression from complementary DNA of skeletal muscle ryanodine receptor. *Nature* **339:**439–445

Tanabe, T., Beam, K.G., Adams, B.A., Niidome, T., Numa, S. 1990*a*. Regions of the skeletal muscle dihydropyridine receptor critical for excitation-contraction coupling. *Nature* **346:**567–569

Tanabe, T., Beam, K.G., Powell, J.A., Numa, S. 1988. Restoration of excitation-contraction coupling and slow calcium current in dysgenic muscle by dihydropyridine receptor complementary DNA. *Nature* **336:**134–139

Tanabe, T., Mikami, A., Numa, S., Beam, K.G. 1990*b*. Cardiac-type excitation-coupling in dysgenic skeletal muscle injected with cardiac dihydropyridine receptor cDNA. *Nature* **344:**451–453

Towbin, H., Staehelin, T., Gordon, J. 1979. Electrophoretic transfer of proteins from polyacrylamide gels to nitrocellulose sheets: Procedure and some applications. *Proc. Natl. Acad. Sci. USA.* **76:**4350–4354

Varsanyi, M., Messer, M., Brandt, N.R., Heilmeyer L.M.G., Jr. 1986. Phosphatidylinositol 4,5-bisphosphate formation in rabbit skeletal and heart muscle membranes. *Biochem. Biophys. Res. Commun.* **138:**1395–1404

Wray, W., Boulikas, T., Wray, V.P., Handock, R. 1981. Silver staining of proteins in polyacrylamide gels. *Anal. Biochem.* **118:**197–203

Received 16 December 1991; revised 8 April 1992